Hydrol. Earth Syst. Sci. Discuss., 6, 207–241, 2009
www.hydrol-earth-syst-sci-discuss.net/6/207/2009/

Hydrology and Earth System Sciences Discussions

Papers published in *Hydrology and Earth System Sciences Discussions* are under open-access review for the journal *Hydrology and Earth System Sciences*

An inversion method based on multi-angular approaches for estimating bare soil surface parameters from RADARSAT-1

M. R. Sahebi[1] and J. Angles[2]

[1]Geomatics Engineering Faculty, K. N. Toosi University of Technology, Tehran, Iran
[2]EADS System and Defence Electronics, Velizy Villacoublay, France

Received: 4 November 2008 – Accepted: 14 November 2008 – Published: 7 January 2009

Correspondence to: M. R. Sahebi (sahebi@kntu.ac.ir)

Published by Copernicus Publications on behalf of the European Geosciences Union.

Abstract

The radar signal recorded by earth observation (EO) satellites is known to be sensitive to soil moisture and soil surface roughness, which influence the onset of runoff.

This paper focuses on the inversion of these parameters using a multi-angular approach based on RADARSAT-1 data with incidence angles of 35° and 47° (in mode S3 and S7). This inversion was done based on three backscatter models: Geometrical Optics Model (GOM), Oh Model (OM) and Modified Dubois Model (MDM), which are compared in order to obtain the best configuration. For roughness expressed in rms of heights, mean absolute errors of 1.23 cm, 1.12 cm and 2.08 cm, and for dielectric constant, mean absolute errors of 2.46, 4.95 and 3.31 were obtained for the MDM, GOM and the OM simulation, respectively. This means that the MDM provided the best results with minimum errors. Based on these results, the latter inversion algorithm was applied on the images and the final results are presented in two different maps showing pixel and homogeneous zones for surface roughness and soil moisture.

1 Introduction

Synthetic Aperture Radars (SAR) are active microwave sensors that have the capability of acquiring data under almost any meteorological conditions and without an external source of illumination. It is therefore possible to collect information on a regular basis over an area often covered by clouds either day or night. This advantage over sensors operating in the visible and the infrared portion of the electromagnetic spectrum improves the capability for monitoring dynamic phenomena. The potential of SAR data has been demonstrated for monitoring the earth's surface (Ulaby et al., 1978, 1982, 1996; Dobson and Ulaby, 1986a, b; Engman and Wang, 1987; Oh et al., 1992; Fung and Chen, 1992; Fung, 1994; Dubois et al., 1995). However, it is sometimes difficult to separate land cover information using a single channel of SAR data. A multi-technique approach using SAR data is thus seen as essential in environmental studies.

HESSD

6, 207–241, 2009

In the scope of this paper, the monitoring of land surface parameters is performed through the estimation of soil surface roughness and moisture status over a large area. Mapping of soil surface roughness and moisture at a large scale regularly or at critical times (floods, droughts, landslides, etc.) is useful for agronomists and hydrologists. It provides an overall view of land surface parameters on a spatial scale. It allows the detection of dry and wet areas, as well as smooth and rough areas and the identification of areas of potential hydrological or agronomic problems. However, soil moisture and soil surface roughness both have an influence on radar backscatter. Moreover, it is important to be able to separate moisture from roughness on the radar signal over bare soils.

Mapping of surface characteristics can be done either from point measurements or estimated values from models and remote sensing. Soil moisture obtained from remote sensing instruments is derived by converting the detected dielectric constant into volumetric water content. On point measurement, remote sensing data are not as accurate as ground point data because of the resolution of the sensors and the algorithms or models that have to be applied to the signal in order to obtain the soil moisture or roughness estimate. However, they do provide information on the spatial variability (Benallegue et al., 1998) and the derived values provide a map of an area without having to interpolate data as with point measurements.

Based on simulation results, Sahebi et al. (2001, 2002) indicated that a multi-angular approach is better adapted for the separation of moisture and roughness signals than multi-polarization and multi-frequency approaches. Therefore, the Radarsat-1 satellite with its capability of acquiring data at different incidence angles can be used for estimating soil moisture and surface roughness. However, it is necessary to develop a method adapted to RADARSAT-1 data for estimating these parameters.

The objective of this paper is to formulate and define a transformation approach to solve the inverse problem for the operational retrieval and mapping of soil surface roughness and moisture. The strategy consists in formulating the inverse problem in the context of multi-angular RADARSAT-1 data. We shall study the relation between the

C-band radar response and soil parameters, specifically the soil dielectric constant (ε) and rms height (s), which are used as constraining target parameters in the Geometrical Optics Model (GOM) (Ulaby et al., 1982), the Oh Model (OM) (Oh et al., 1992) and the Modified Dubois Model (MDM) (Angles, 2001). Based on the results obtained with the MDM, a roughness and a moisture map for the Chateauguay watershed (Quebec, Canada) were produced.

2 Study site and data description

The agricultural site chosen for this study is part of the Chateauguay watershed (73°46′ W, 45°19′ N), located on the south shore of the St. Lawrence River, southwest of Montreal, Canada (Fig. 1). The area consists mainly of agricultural fields on a rather flat relief plateau with homogeneous texture composed of about 36% clay, 42% silt and 22% sand. During the ground surveys the parcel surfaces were rough to very rough.

Roughness and moisture measurements were carried out over 27 agricultural parcels simultaneously with the image acquisitions (Fig. 2). Roughness measurements were made using a homemade needle profilometer measuring 2 m in length. To calculate rms height, six 2 m long (1.5 cm sampling interval) surface profiles (three parallel and three perpendicular to the soil furrows) were investigated for each parcel. These profiles were photographed and then digitized. The method for extracting and modeling the roughness parameters such as rms height and correlation length has been described in detail by Beaulieu et al. (1995).

Soil surface moisture measurements were carried out with a Thetaprobe soil moisture sensor, based on the time domain reflectometry (TDR) (Delta Devices Ltd., 1996) concept. The measurements reflect moisture in the 0–5 cm depth corresponding to the length of the Thetaprobe needles. Fifteen samples were taken in each parcel of land. Using the equation presented in the Thetaprobe Soil Moisture User Manual (Delta Devices Ltd., 1996), the direct outputs (DC voltage in V) were converted to both volumetric soil moisture content ($m^3\ m^{-3}$) and dielectric constant. Also, to evaluate the results obtained with this method, five 0–5 cm soil samples for each parcel were transferred to our laboratory. Wet and dry weights were used to determine gravimetric and volumetric soil moisture content. The soil moisture contents ($m^3\,m^{-3}$) obtained by these two methods were compared and a mean relative difference of 12% (equivalent to 1.8% in volumetric soil moisture) was observed between the two methods.

The satellite data used in this study correspond to a RADARSAT-1 image pair. The first image was acquired on 15 November 1999 in S3 (Standard-3) mode with incidence angles ranging from 30 to 35° and, the second image was acquired on 18 November 1999 in S7 (Standard-7) mode with incidence angles ranging from 45 to 49°. The RADARSAT DN values were converted to backscattering coefficient (σ^0) according to Shepard (1998). In order to include the spatial variability and to avoid problems related to georeferencing of individual pixels of the parcels in the study area (homogeneous soil structure, bare soil, homogeneous ploughing), an average σ^0 (dB) was assigned to each parcel (approximately 20 to 30 pixels). The surface roughness and moisture were measured in-situ on 15 and 18 November (the same dates as the satellite image acquisitions). Between the periods of data acquisition, the weather was stable and surface moisture had not changed significantly because of the low evaporation and temperature at that time of the year. According to local observations and Environment Canada, average daily temperatures were 2.3°C (with a minimum value of 1.5° and a maximum value of 7°) and there was no recorded rainfall nor ground frost between the two acquisition dates. However, to completely satisfy the conditions of this study, we selected 20 parcels that had nearly the same moisture and roughness for the two dates.

3 Methodology

The important parameters that significantly influence the soil surface radar response may be classified into two categories: 1) the target parameters such as moisture, roughness and vegetation cover (if present) and, 2) the sensor parameters such as frequency, polarization and incidence angle. Usually in remote sensing applications, the sensor parameters are known; however, the relationship between the target and the measured signals have to be investigated. Estimation of soil surface parameters was usually obtained by using theoretical or empirical relationships to convert the measured backscatter coefficient (σ^0) into soil surface roughness and moisture (Dobson and Ulaby, 1986a; Prévot et al., 1993; Ulaby et al., 1996). Thus for each target, we had one equation with two unknowns, or three if the model incorporates the correlation length. As a consequence, the use of radar data acquired with a single configuration does not generally allow the estimation of these soil surface variables. Therefore, to simultaneously estimate the surface parameters over complex areas, multi-technique concepts (multi-polarization, multi-angular, multi-sensor, multi-frequency, and multi-temporal) are the main solution.

From a ground based experiment (Chanzy et al., 1998) and a theoretical study (Sahebi et al., 2001, 2002), it was demonstrated that the multi-angular configuration is the best to estimate bare soil surface parameters from. For this reason, the multi-angular configuration is used for the inversion of backscattering models to estimate roughness and soil moisture from RADARSAT-1 data acquired at two different incidence angles. It has to be noted that this approach was tested with different RADARSAT-1 images acquired at different incidence angles (between 20 and 49°) and the images presented gave the optimal results.

3.1 Model descriptions

As mentioned before, the aim of this study is to estimate bare soil surface parameters using multi-angular approaches. This process was carried out using existing theoretical and empirical backscatter models that introduce the relationship between backscatter coefficient and surface parameters (roughness and dielectric constant).

Considering that the study site profiles contain very rough surfaces, the comparison of the mentioned backscattering models is carried out using simulations by GOM (Geometrical Optics Model; Ulaby et al., 1982), OM (Oh Model; Oh et al., 1992) and MDM (Modified Dubois Model; Angles, 2001).

HESSD

6, 207–241, 2009

3.1.1 Geometrical Optics Model (GOM)

The Geometrical Optics Model (GOM) also known as the Kirchhoff method under the stationary phase approximation intended to express scattering by rough surfaces with, $0.06k^2\ell^2>ks$, $k\ell>6$ and $(2ks.\cos\theta^2>10$ where ℓ is the correlation length, k is the wave number ($k=2\pi/\lambda$, where λ is the wavelength), s is the root mean square (rms of heights) and θ is the incidence angle. This model predicts that $\sigma^0_{hh}(\theta)=\sigma^0_{vv}(\theta)$, at all incidence angles of the radar signal. The expression for the co-polarized backscattering coefficient is given by:

$$\sigma^0_{pp}(\theta)=\left[\frac{\left|R_{pp}(0)\right|^2}{(2\mathrm{m}^2\cos^4\theta)}\right]\times\exp\left(\frac{\tan^2\theta}{2\mathrm{m}^2}\right) \tag{1}$$

where $R_{pp}(0)$ is the surface reflectivity from normal incidence and m is the rms slope of the surface and is equal to $\sqrt{2}s/\ell$ and s/ℓ for Gaussian and exponential functions respectively (Oh et al., 1992). According to Oh et al. (1992), the exponential function is adapted to smooth surfaces and the Gaussian autocorrelation function is adapted to rough surfaces. Based on the study area descriptions (rough to very rough surfaces), the Gaussian autocorrelation function was chosen for calculating m values.

3.1.2 Oh Model (OM)

Because of the inadequate performance of theoretical models for predicting the backscatter response of random surfaces, Oh et al. (1992) developed an empirical model based on experimental data acquired in L- C- and X-bands (1.5, 4.75 and 9.5 GHz, respectively). This model was designed for surfaces with various moisture conditions and roughnesses, from slightly smooth to very rough and does not incorporate the correlation length. The valid surface conditions cover the following ranges: $0.1<ks<6.0$, $2.6<k\ell<19.7$ and $9\%<m_v<31\%$, where m_v is the volumetric soil moisture. The backscattering coefficients in HH polarization for this model can be expressed by:

$$\sigma^0_{hh} = g\sqrt{p}\cos^3\theta\,[\Gamma_v(\theta) + \Gamma_h(\theta)] \tag{2}$$

where $\sqrt{p}=1-\left(\frac{2\theta}{\pi}\right)^{[1/3\Gamma_0]} \times \exp(-ks)$ and $g = 0.7[1-\exp(-0.65(ks)^{1.8})]$ and Γ_0 is the Fresnel reflectivity of surface at nadir; Γ_v and Γ_h are the Fresnel reflection coefficients for horizontal and vertical polarization, respectively. Correlation length effect is not taken into account.

3.1.3 Modified Dubois Model (MDM)

The empirical model developed by Dubois et al. (1995) was initially developed in order to separate moisture and roughness using a bipolarization approach. This model is limited to $ks \leq 2.5$, $\theta \geq 30^{\circ}$ and moisture contents $m_v \leq 35\%$. This model was tested over the study area by researchers at Université de Sherbrooke (Angles, 2001; Angles et al., 2002) and the results showed an important difference between simulated and measured values of moisture and roughness. The method that Dubois et al. (1995) followed was used for adapting the Dubois model into measured data over the Quebec agricultural area. To overcome this discrepancy, the RADARSAT-1 data (C-band, HH-polarized and incidence angles between 20° and 50°) and measured ground data (soil surface roughness, soil moisture and soil texture) were used. This modification is presented as a new model referred to as the Modified Dubois Model (MDM). It expresses the backscattering coefficient for this model and is described by Eq. (3) that can be applied to bare agricultural surfaces in Quebec with $1\,\text{cm} < s < 6\,\text{cm}$ and $14\% < m_v < 32\%$ (Angles, 2001).

$$\sigma^0_{hh} = 10^{-3.67} \times \frac{\cos^{1.5}\theta}{\sin^5\theta} \times 10^{0.112\tan\theta\,\varepsilon} \times (ks.\sin\theta)^{0.883} \times \lambda^{0.7} \tag{3}$$

where k is the wave number ($k = 2\pi/\lambda$) and λ is the wavelength.

Applying this model to RADARSAT-1 data acquired at two different incidence angles of the same target with a short time interval, this approach generates a two equation system with two unknowns, which can be resolved to obtain s and ε. However, for validation purposes, this model should be tested in other regions with different conditions.

4 Inversion method

Let us suppose that we have backscatter coefficient (σ^0_{hh} in this case) measurements for a given surface at the given incidence angles θ_1, θ_2 and θ_3 (if applicable). From these measurements, it is possible to compute the land-surface parameters by inverting the above models.

As explained, three models were chosen. The MDM is analytically invertible. Equations (4) and (5) show the inversion of this model to calculate land-surface parameters using the multi-angular approach for hh-polarization:

$$\varepsilon_r = \frac{\log[A]}{0.112\times(\tan\theta_1 - \tan\theta_2)} \tag{4}$$

$$s = \frac{1}{k}\times\sqrt[0.883]{10^{3.67}\times\sigma^0_{HH}(\theta_1)\times\frac{\sin^{4.117}(\theta_1)}{\cos^{1.5}(\theta_2)}\times A^{-\left(\frac{\tan(\theta_1)}{\tan(\theta_1)-\tan(\theta_2)}\right)}\times\lambda^{-0.7}} \tag{5}$$

where $\sigma^0_{hh}(\theta_1)$ and $\sigma^0_{hh}(\theta_2)$ are the backscatter coefficients measured at θ_1 and θ_2, respectively, and:

$$A = \frac{\sigma^0_{HH}(\theta_1)\times\sin^{4.117}(\theta_1)\times\cos^{1.5}(\theta_2)}{\sigma^0_{HH}(\theta_2)\times\sin^{4.117}(\theta_2)\times\cos^{1.5}(\theta_1)} \tag{6}$$

The OM and GOM are not invertible by this way. For these models, the Newton-Raphson method (Ortega and Rheinboldt, 1970), a numerical iterative method, is used in the retrieval algorithm to solve the inverse problem.

Based on the Newton-Raphson method, the variable matrices (the unknown variables) are s and ε_r for OM and s, ε_r and ℓ for GOM. The known parameters in the model are the backscatter coefficients at two or three different incidence angles. The algorithm can be summarized as follows:

Step 1. Presentations of the zeroed functions (f_i) are issued by using GOM and OM based on the multi-angular approach. For example, these functions for OM are:

$$f_1 = \sigma^0_{hh}(\theta_1) - g\sqrt{p}\cos^3\theta_1[\Gamma_v(\theta_1) + \Gamma_h(\theta_1)] = 0 \tag{7a}$$

$$f_2 = \sigma^0_{hh}(\theta_2) - g\sqrt{p}\cos^3\theta_2[\Gamma_v(\theta_2) + \Gamma_h(\theta_2)] = 0 \tag{7b}$$

(p and g functions are already explained in Eq. 2).

Step 2. Computation of the error matrix based on an initial guess of the variables (ε_r and s for OM; ε_r, s and ℓ for GOM). In this study, the initial values were: ε_r=10, s=3 cm and ℓ=5 cm.

Step 3. Computation of the matrix α_{ij} which is the relation between the backscatter coefficient and the soil surface parameters. Equations 8 and 9 present this matrix for OM and GOM respectively:

$$\text{for OM} \quad \alpha = \begin{bmatrix} \frac{\partial f_1}{\partial s} & \frac{\partial f_1}{\partial \varepsilon_r} \\ \frac{\partial f_2}{\partial s} & \frac{\partial f_2}{\partial \varepsilon_r} \end{bmatrix} \tag{8}$$

$$\text{for GOM} \quad \alpha = \begin{bmatrix} \frac{\partial f_1}{\partial s} & \frac{\partial f_1}{\partial \varepsilon_r} & \frac{\partial f_1}{\partial \ell} \\ \frac{\partial f_2}{\partial s} & \frac{\partial f_2}{\partial \varepsilon_r} & \frac{\partial f_2}{\partial \ell} \\ \frac{\partial f_3}{\partial s} & \frac{\partial f_3}{\partial \varepsilon_r} & \frac{\partial f_3}{\partial \ell} \end{bmatrix} \tag{9}$$

Step 4. Calculation of the error (δx_j) in the estimation of land surface properties. This matrix can be solved by the LU (Lower and Upper triangular) decomposition method (Westlake, 1968).

Step 5. Correction of the error in the estimation of soil surface parameters by δx_j for the next iteration.

Step 1 through 5 are repeated until convergence is reached; that is, δ=10^{-5} in this case.

HESSD

6, 207–241, 2009

Bare soil moisture and roughness estimation

M. R. Sahebi and J. Angles

4.1 Evaluation of the results

Evaluation of the errors requires comparisons between predicted and measured surface parameters. All comparisons between measured in-situ and predicted surface parameters obtained by RADARSAT-1 images are presented on an even basis for rms heights and surface dielectric constants (separately). They are carried out using the coefficient of performance CP'_A (James and Burgess, 1982):

$$CP'_{\dot{A}} = \sum_{i=1}^{n} (S(i) - O(i))^2 \Big/ \sum_{i=1}^{n} \left(O(i) - O_{\text{avg}}\right)^2 \tag{10}$$

where $O(i)$ is the i_{th} observed parameter, O_{avg} is the mean value of the observed parameter, $S(i)$ is the i_{th} predicted parameter using radar images and n is the total number of events. The coefficient of performance approaches zero as observed and predicted values get closer. This coefficient can show the efficiency of each model for estimating surface parameters. In this study, the mean total absolute error for the results of each model is also calculated.

5 Results and discussion

Figures 3 to 8 present a comparison between the value of surface parameters estimated from the inversion of radar data and those measured in-situ. For rms height, the results with minimum error are given by GOM with a mean absolute error of 1.12 cm, followed by MDM (with a mean error equal to 1.23 cm) and OM (with a mean error equal to 2.08 cm). However, for the dielectric constant, MDM definitely has the best estimation with an error equal to 2.46 followed by OM (with an error equal to 3.35) and GOM (with an error equal to 4.59). As explained, to be able to compare these results, we also used the coefficient of performance (CP'_A). Table 1 presents the values of this coefficient. These results show that the inversion of MDM gives the best results for estimating the soil surface parameters.

HESSD

6, 207–241, 2009

For MDM and OM, the estimation of the dielectric constant is more exact than the estimation of rms height. Contrarily, the rms height estimated by GOM is more exact. On the other hand, for GOM, total values of CP'_A, for the dielectric constant are greater than those for rms height (Table 1). This sensitivity to roughness may be explained by the behavior of GOM. According to this model, the statistical variation of surface roughness is characterized by its rms height, correlation length and correlation function that is represented by rms slope (m) in Eq. (1). Therefore, the accuracy of the roughness estimation also depends on the estimation of correlation length. However in MDM and OM, roughness is characterized only by rms height.

This study presents an approach to estimate surface parameters derived from SAR satellite data with reduced estimation errors, compared to other studies. However, there are still errors in the estimation of soil surface parameters. Further investigations are needed to understand this drawback, but several possibilities can already be suggested:

- Failure of the models to present a real relationship between radar signal properties and target parameters: unfortunately, none of the backscatter models provides results in good agreement with experimental observations for all of the polarization configurations and over a wide range of incident angles, even when confined to its presumed validity range (Henderson and Lewis, 1998).

- Behavior of the models in the multi-angular approach context to find an exact solution: Consider the case of two dimensions, where we want to simultaneously solve:

  $$\begin{cases} f1 : f_{\theta_1,\sigma^0}(\varepsilon, s) = 0 \\ f2 : f_{\theta_2,\sigma^0}(\varepsilon, s) = 0 \end{cases}$$

  An example of this case is presented by Eq. (7a) and (b) for OM. Each of the functions has zero regions where their respective functions are positive to negative. Unfortunately, according to the model behavior, the functions f_1 and f_2 are not dependent on each other. Note further that the zero contours consist of a number of disjointed closed curves. Figure 9 showing the curves ε vs. s for parcel no 120 (σ_1^0=−10.07 dB and σ_2^0=10.77 dB for θ_1=35° and θ_2=47.4°, respectively) simulated by OM is an example of this situation. The solution obtained with these data was the point with the coordinate s=2.32 cm and ε=5 that was the closest point between the two curves. This phenomenon was also observed in some cases in the inversion with GOM. Figure 10 shows the same curves simulated by MDM. These curves intersect exactly at s=3.25 cm and ε=11.75 which is the exact solution of the system of equations.

- Incompatibility between ground measurements and estimated parameters: as explained, the ground data for each parcel are issued by some point measurements and their mean are presented as rms height and dielectric constant of the parcel. These measurements were random and numerous enough to calculate a good mean value, but generally, can this method present the true characterization of the surface parameters? Unfortunately, no better method for this measurement has yet been presented.

- Error in the estimation of the backscatter coefficient for parcels. To present the backscatter coefficient of each parcel, we calculated a mean of the pixels that were within the parcels. The pixel values vary sometimes with considerable variance. This operation increases errors.

- Influence of tillage direction and look direction: the orientation of mechanical tillage, which can be related to roughness measurements, has an influence on backscattering signals (Remond et al., 1999; Smyth et al., 2000). However, the backscatter models do not enable the simulation of this influence directly. Also, the use of images acquired at different orbits (ascending and descending) is sometimes inevitable in temporal studies with SAR data. The look direction accounted for a 1.5 dB difference in σ^0 for ERS-1 images by Gauthier et al. (1998). Smyth et al. (2000) obtained maximum 2 dB difference in σ^0 for RADARSAT-1.

- Influence of speckle and climatic conditions on radar signals. Discussion of these problems is not the aim of this paper. However, these phenomena can produce some errors when calculating backscatter coefficients from satellite images.

5.1 Surface parameter mapping

The inversion algorithm using the MDM model is applied on two RADARSAT-1 images of the watershed under study. Two important points should be noted, first, forest and urban areas are masked on the maps; second, the humidity maps are presented in terms of volumetric soil moisture ($m^3\,m^{-3}$) obtained by inverting the empirical model of the dielectric constant developed by Halikainen et al. (1985). This application was carried out at two different scales namely pixel scale and homogeneous zone scale. At pixel scale (Figs. 11 and 12), the inversion is applied directly on the two images pixel by pixel. The speckle in the images was reduced using Lee filtering (Lee, 1981). The pixel scale maps are more accurate, however the pixel values vary and are also difficult to use, so it is difficult to have a general idea of the surface parameter distribution over the watershed. To solve this problem, we used the homogeneous zone scale. Each homogeneous zone on a radar image presents a minimal variance in the backscatter coefficients. Furthermore, within an homogeneous zone the physical characteristics of the soil surface are almost the same. This kind of presentation allows us to have a general view of surface parameter distribution (Figs. 13 and 14).

Creating an homogeneous zone comprises four steps:

1) Improving the image contrast: contrast is only for providing better viewing of the images and does not modify the pixel values. This step helps to get a better view of the images specially for manual digitization (step 3).

2) Noise reduction: this step is carried out using despeckle filters. Generally, the adaptative filters like Lee or Frost filters reduce noise notably. In this study, the Lee filter and a low-pass filter were tested. As expected, the Lee filter reduced speckle better than low-pass filter, but it modified the pixel values and that changed the

final results. On the contrary, the low-pass filter reduced noise less than the Lee filter but the pixel values did not change significantly. However, the final results (homogeneous zone maps) were approximately the same. Therefore, the best filter should be chosen in each case. For this study, it was the low-pass filter.

3) Edge detection of homogeneous zones: in this step, two filters were used to delimit the homogeneous zones based on the minimal variance of σ^0 in each zone (Angles, 2001), and then the edge of each zone was detected using an edge detection filter. For a few zones, the edge polygon was not correctly closed. This problem was corrected manually.

4) Averaging: in the last step, the average of the $\sigma^0 s$ in each zone was calculated and presented as the σ^0 value of the homogeneous zone. Figure 15 presents the methodological flowchart for homogeneous zone calculation.

6 Conclusions

This work has demonstrated the possibility of using the multi-angular approach to derive soil moisture and surface roughness from a pair of RADARSAT-1 images. In spite of some errors, this estimation derived from satellite radar data is a potentially useful tool for estimating soil surface parameters over extended areas. These errors can be produced either by some essential averaging or by the behavior of the backscattering models or the incompatibility of the ground measurements and the results obtained using satellite images. However, in this paper, we demonstrated that using the multi-angular approach, it is possible to decrease these types of errors and derive acceptable results for the overall watershed area.

To minimize the influence of backscatter models, we used the Modified Dubois Model (MDM) developed for agricultural sites in Quebec and presenting minimum errors. This result is obtained by comparing the same results calculated by GOM, MDM and OM.

HESSD

6, 207–241, 2009

From an applications point of view, the final products of this investigation are soil surface parameter maps. These maps were produced at two different scales that can serve for many applications like hydrological models, agricultural or environmental management, etc. For example, the pixel scale maps of moisture and roughness can readily be used in hydrological models based on pixel like units such as AGNPS (Young et al., 1987) or ANSWERS (Beasley et al., 1980). However the homogeneous zone maps present the soil surface distribution in a large area and can be used in agricultural or hydrological management at the subcatchment scale by hydrological response units such as those used in the SWAT (Soil and Water Assessment Tool) model (Arnold et al., 1993). However, there are still two major limitations to this approach for an operational use in hydrology. First, hydrological models use roughness parameters such as Manning coefficients or Curve Numbers which are not directly linked to rms of height, a correspondence table should be developed. Second, acquisition conditions for multi angular RADARSAT-1 data can often imply several days between the two images. Soil moisture and roughness can change between the two dates (rain, strong evaporation, ploughing, etc.). This situation should however improve with RADARSAT-2 or multi sensor approaches such as a combination of RADARSAT-1 and ENVISAT images.

Acknowledgements. This study was leaded by Ferdinand J. Bonn (1943–2006) who was an outstanding researcher, a terrific teacher, and simply put a wonderful man. Also this work partly supported by FCAR (Action Concertée Radarsat) and NSERC. The authors want to thank all the colleagues of CARTEL, especially P. Gagnon, G. Bennié, R. Magagi and D. C. He, for their helps and editing work.

References

Angles, J.: Séparation de l'humidité et de la rugosité dans le signal retrodiffusé des images RSO selon une approche multi-angle, Mémoire de Maîtrise, Dép. de géographie et télédétection, Université de Sherbrooke, Canada, 82 pp., 2001.

Arnold, J. G., Allen, P. M., and Bernhardt, G.: A comprehensive surface-groundwater flow model, J. Hydrol., 142, 47–69, 1993.
Beasley, D. B., Huggins, L. F., and Monke, E. J.: ANSWERS: A model for watershed planning, T. ASAE, 23(4), 938–944, 1980.
Benallegue, M., Taconet, O. Vidal-Madjar, D., and Normand, A.: The use of radar backscattering signals for measuring soil moisture and surface roughness, Remote Sens. Environ., 53, 61–68, 1998.
Chanzy, A., King, C., Prévot, L., and Remond, A.: Comparison of ERS and RADARSAT measurements on bare soils, first results, Second Int. Workshop on Retrieval of Bio-&Geophysical Parameters from SAR Data, ESTEC, The Netherlands, 471–477, 1998.
Delta Devices Ltd.: Thetaprobe soil moisture sensor, User manual, MI1-UM-2, Delta Devices Ltd, UK, 18 pp., 1996.
Dobson, M. C. and Ulaby, F. T.: Active microwave soil moisture research, IEEE T. Geosci. Remote, 24(1), 23–36, 1986a.
Dobson, M. C. and Ulaby, F. T.: Preliminary evaluation of the SIR-B response to soil moisture, surface roughness, and crop canopy cover, IEEE T. Geosci. Remote, GE-24(4), 517–526, 1986b.
Dubois, P. C., van Zyl, J., and Engman, T.: Measuring soil moisture with imaging radars, IEEE T.n Geosci. Remote, 33(4), 915–926, 1995.
Engman, E. T. and Wang, J. R.: Evaluation Roughness Models of Radar Backscatter, IEEE T. Geosci. Remote, GE-25(6), 709–713, 1987.
Fung, A. K.: Microwave scattering and emission models and their applications, Norwood: Artech House, 573 pp., 1994.
Fung, A. K. and Chen, K. S.: Dependence of the surface backscattering coefficients on roughness, frequency and polarization states, Int. J. Remote Sens., 13(9), 1663–1680, 1992.
Gauthier, Y., Bernier, M., and Fortin, J. P.: Aspect and incidence angle sensivity in ERS-1 SAR data, Int. J. Remote Sens., 19(9), 2001–2006, 1998.
Halikainen, M. T., Ulaby, F. T., Dobson, M. C., El-Rays, M. A., and Wu, L.: Microwave dielectric behavior of wet soil – Part I – Empirical models and experimental observations, IEEE T. Geosci. Elect., GE-23(1), 25–34, 1985.
Henderson, F. M. and Lewis, A. J.: Principles and applications of imaging radar, John Wiley & Son Inc., 3rd edn., Chapter 8, 1074 pp., 1998.

James, L. D. and Burgess, S. J.: Selection, calibration and testing of hydrologic models, in: Hydrologic Modeling of Small Watersheds, edited by: Hann C. T., Johnson H. P., and Brakkensiek, D. L., ASAE, St. Joseph, Mich, 437–472, 1982.

Lee, J. S.: Refined filtering of image noise using local statistics, Comput. Vision Graph., 15, 380–389, 1981.

Oh, Y., Sarabandi, K., and Ulaby, F. T.: An empirical model and inversion technique for radar scattering from bare soil surfaces, IEEE T. Geosci. Remote Sens., 30(2), 370–381, 1992.

Ortega, J. M. and Rheinboldt, W. C.: Iterative solution of nonlinear equations in several variables, New York, Academic Press Inc., 572 pp., 1970.

Prévot, L., Champion, I., and Guyot, G.: Estimating surface soil moisture and leaf area index of a Wheat Canopy Using a Dual-Frequency (C and X Bands) Scatterometer, Remote Sens. Environ., 46, 331–339, 1993.

Remond, A., Beaudoin, A., and King, C.: SAR imagery to estimate roughness parameters when modelling runoff risk, Int. J. Remote Sens., 20(13), 2613–2625, 1999.

Sahebi, M. R., Angles, J., and Bonn, F.: A comparison of multi-polarization and multi-angular approaches for estimating bare soil surface roughness from spaceborne radar data, Can. J. Remote Sens., 28(5), 641–652, 2002.

Sahebi, M. R., Angles, J., and Bonn, F.: A multi-angular Radarsat based C-band backscattering model for estimation of bare soil surface roughness, Proceedings of the 23rd Canadian Symposium on Remote Sensing, August, 21–24, 2001, Ste-Foy, Canada, 865–871, 2001.

Shepard, N.: Extraction of beta nought and sigma nought from RADARSAT CDPF products, ALTRIX Systems, Ontario, Canada, Report No: AS97-5001, 12, 1998.

Smyth, J., Bonn, F., Hardy, S., Rémond, A., and Clément, P.: Potential retrieval of tillage direction as a runoff indicator using RADARSAT data, Remote Sensing in Hydrology 2000, AIHS Red book 267, 368–370, 2000.

Ulaby, F. T., Batlivala, P. P., and Dobson, M. C.: Microwave dependence on surface Roughness, soil moisture and soil texture: Part I – bare soil, IEEE T. Geosci. Elect., 16(4), 286–295, 1978.

Ulaby, F. T., Dubois, P. C., and van Zyl, J.: Radar mapping of surface soil moisture, J. Hydrol., 184, 57–84, 1996.

Ulaby, F. T., Moore, R. K., and Fung, A. K.: Microwave remote sensing active and passive, Vol. II, Radar Remote Sensing and Surface Scattering and Emission Theory, Artech House, Ann Arbor Ltd., 457–1064, 1982.

Westlake, J. R.: Handbook of numerical matrix inversion and solution of linear equations, John Wiley & Son Inc., New York, 171 pp., 1968.
Young, R. A., Onstad, C. A., Bosch, D. D., and Anderson, W. P.: Agricultural nonpoint-source pollution model (AGNPS) I and II Model documentation, St. Paul, Minn, Pollution Control Agency, Washington, DC, USDA-ARS, 77 pp., 1987.

HESSD
6, 207–241, 2009

Bare soil moisture and roughness estimation

M. R. Sahebi and J. Angles

Table 1. Mean absolute error and coefficient of performance (CP'_A) for surface parameters obtained by inversion approach.

Models	Errors		CP'_A		
	Height rms (cm)	Dielectric constant	Height rms	Dielectric constant	Total
M D M	1.23	2.46	2.26	1.7	1.98
GOM	1.12	4.59	2.03	6.28	4.16
OM	2.08	3.35	6.30	3.59	4.95

HESSD
6, 207–241, 2009

HESSD

6, 207–241, 2009

Bare soil moisture and roughness estimation

M. R. Sahebi and J. Angles

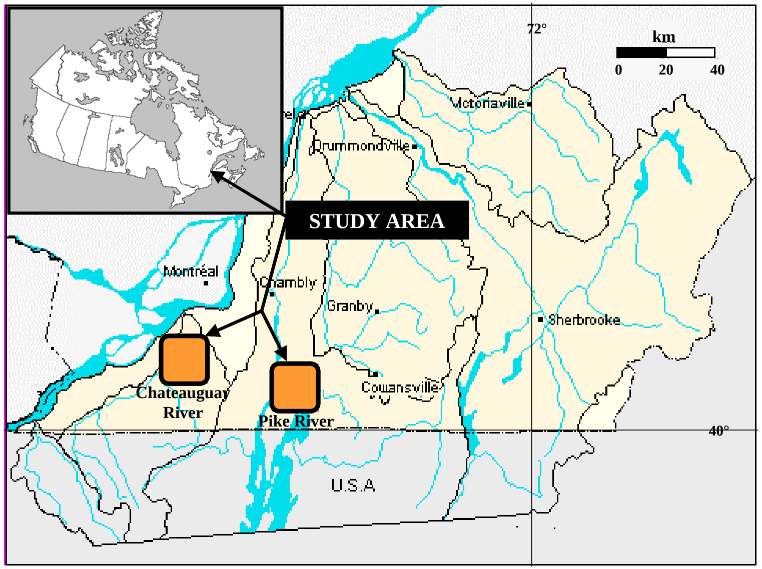

Fig. 1. Location of study area.

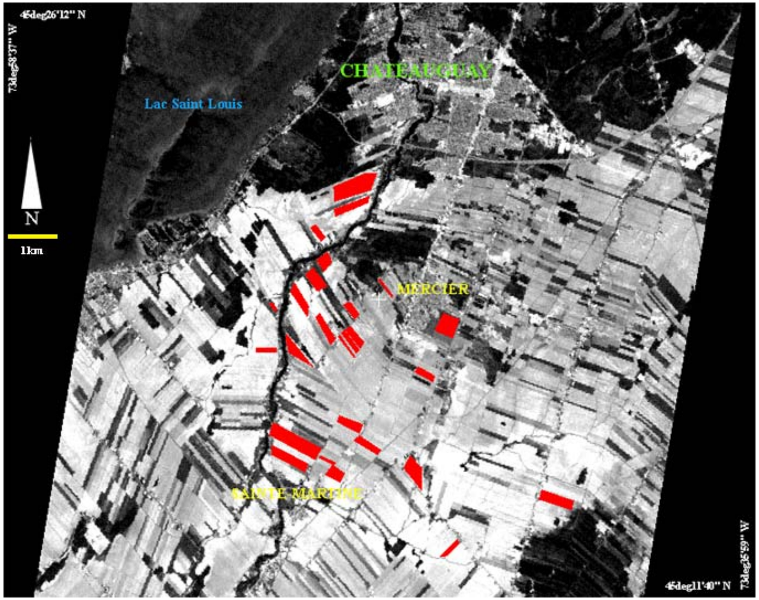

Fig. 2. Location of the parcels (Airborne photography over Chateauguay watershed).

HESSD

6, 207–241, 2009

Bare soil moisture and roughness estimation

M. R. Sahebi and J. Angles

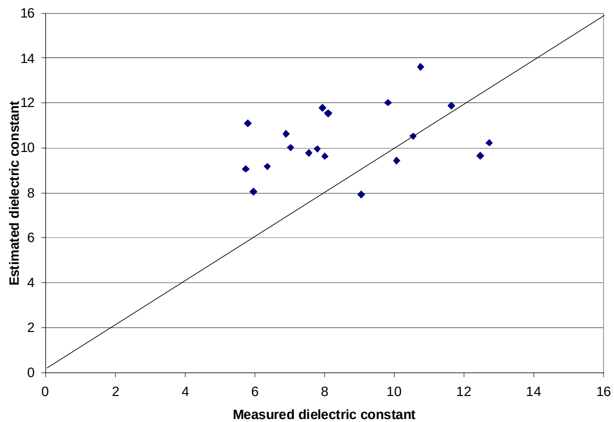

Fig. 3. Scatter plot of dielectric constant measured and estimated by MDM.

HESSD

6, 207–241, 2009

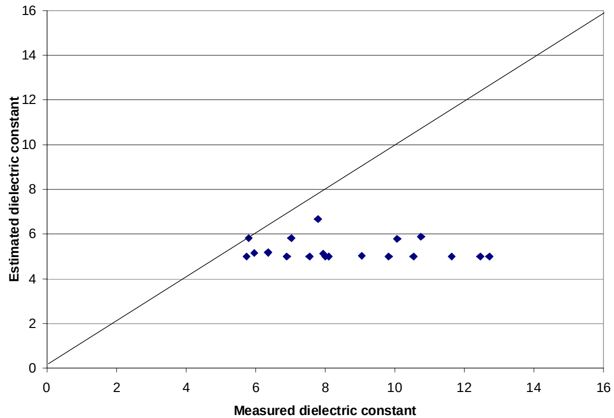

Fig. 4. Scatter plot of dielectric constant measured and estimated by OM.

HESSD
6, 207–241, 2009

Bare soil moisture and roughness estimation

M. R. Sahebi and J. Angles

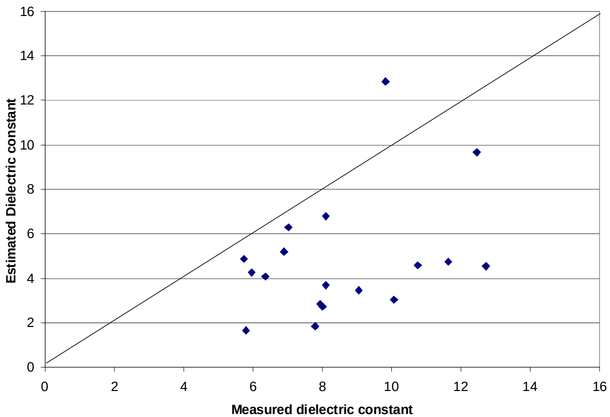

Fig. 5. Scatter plot of dielectric constant measured and estimated by GOM.

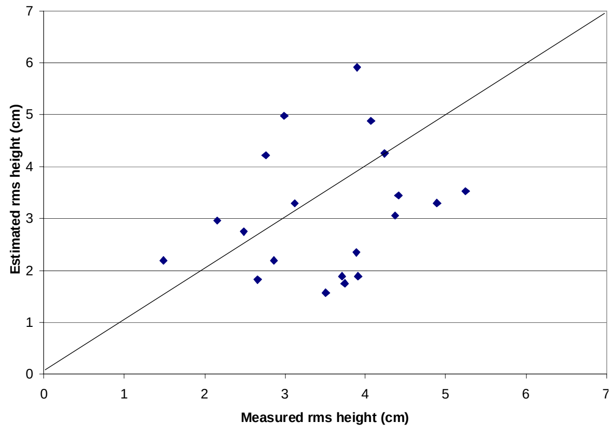

Fig. 6. Scatter plot of rms height measured and estimated by MDM.

HESSD
6, 207–241, 2009

Title Page
Abstract
Introduction
Conclusions
References
Tables
Figures
◄
►
Back
Close
Full Screen / Esc
Printer-friendly Version
Interactive Discussion

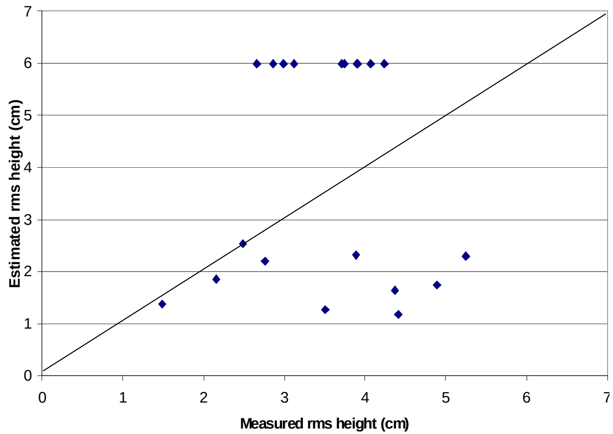

Fig. 7. Scatter plot of rms height measured and estimated by OM.

HESSD
6, 207–241, 2009

Bare soil moisture and roughness estimation

M. R. Sahebi and J. Angles

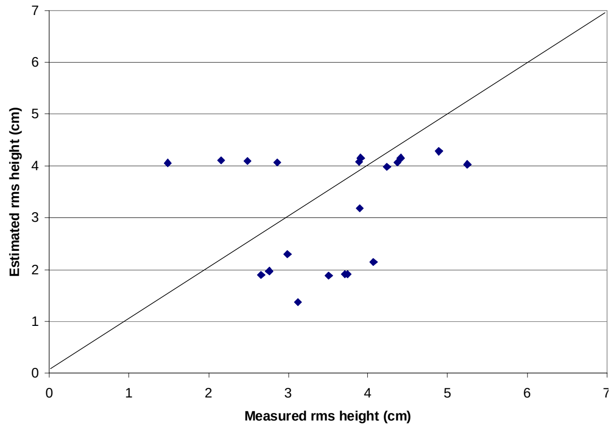

Fig. 8. Scatter plot of rms height measured and estimated by GOM.

HESSD
6, 207–241, 2009

Bare soil moisture and roughness estimation

M. R. Sahebi and J. Angles

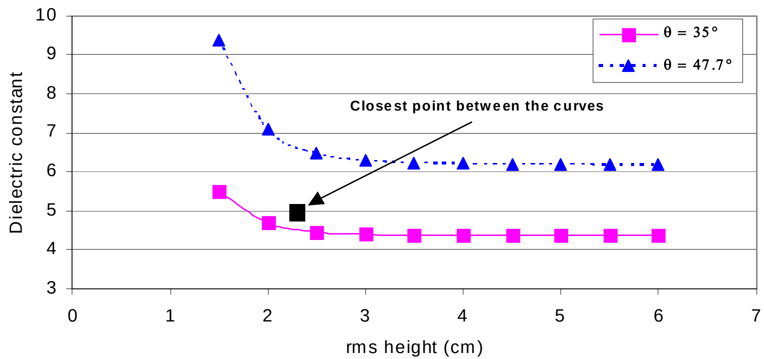

Fig. 9. Variation of the dielectric constant as a function of rms height for two different.

HESSD
6, 207–241, 2009

Bare soil moisture and roughness estimation

M. R. Sahebi and J. Angles

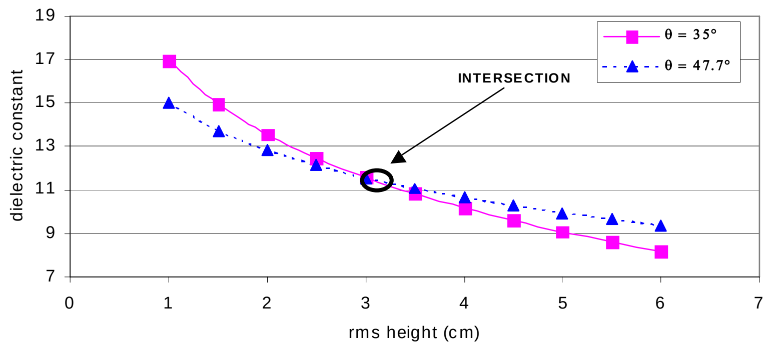

Fig. 10. Variation of the dielectric constant as a function of rms height for two different.

HESSD

6, 207–241, 2009

Bare soil moisture and roughness estimation

M. R. Sahebi and J. Angles

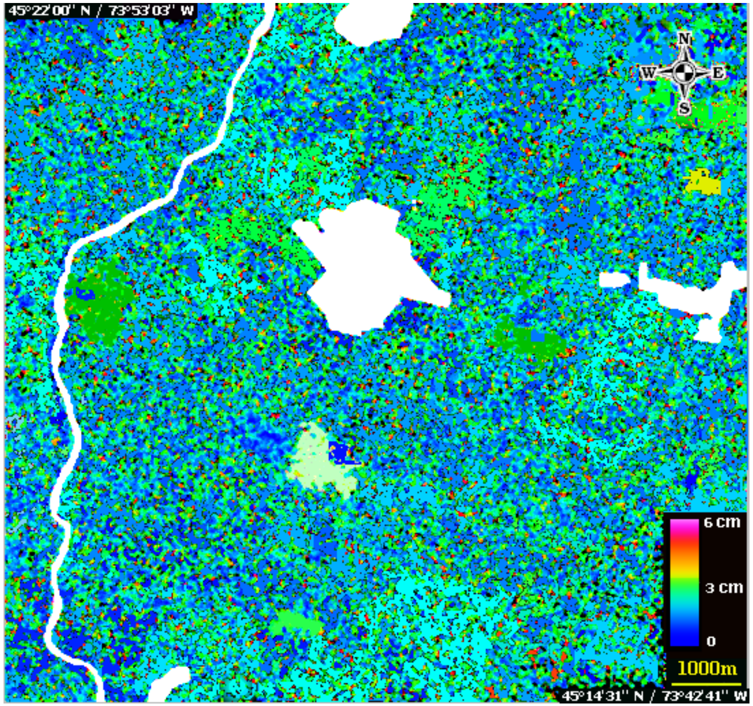

Fig. 11. rms height map at pixel scale.

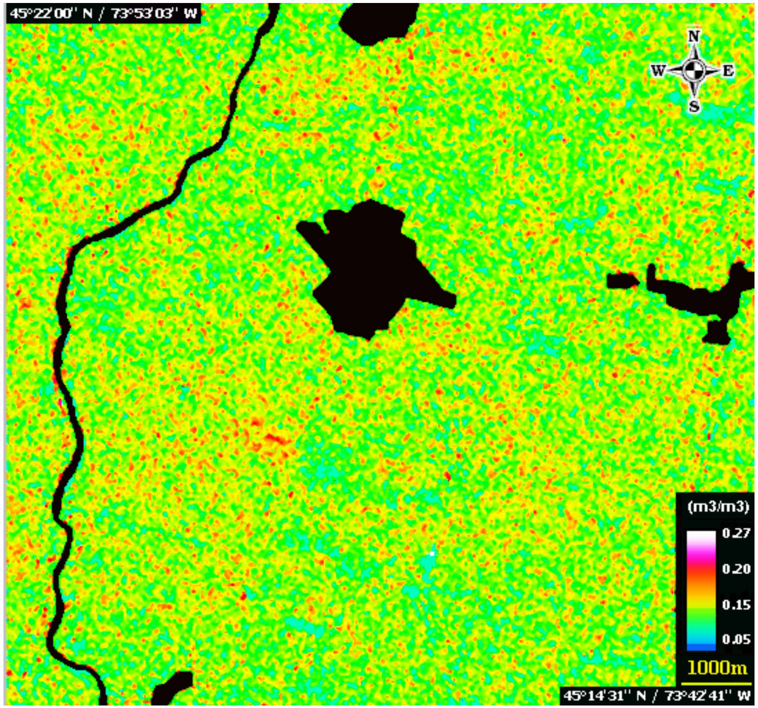

Fig. 12. Volumetric humidity map at pixel scale.

HESSD
6, 207–241, 2009

Bare soil moisture and roughness estimation

M. R. Sahebi and J. Angles

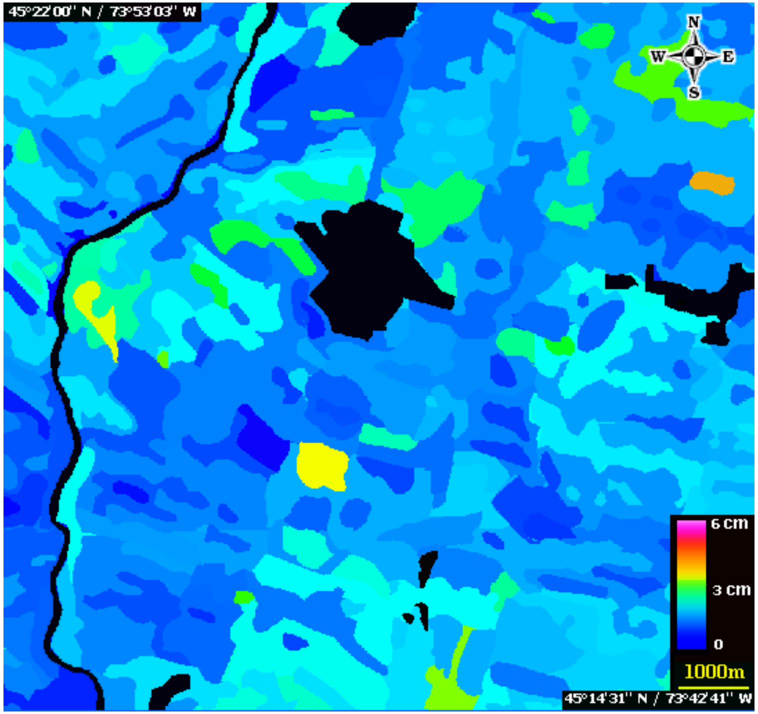

Fig. 13. rms height map in homogeneous zone scale.

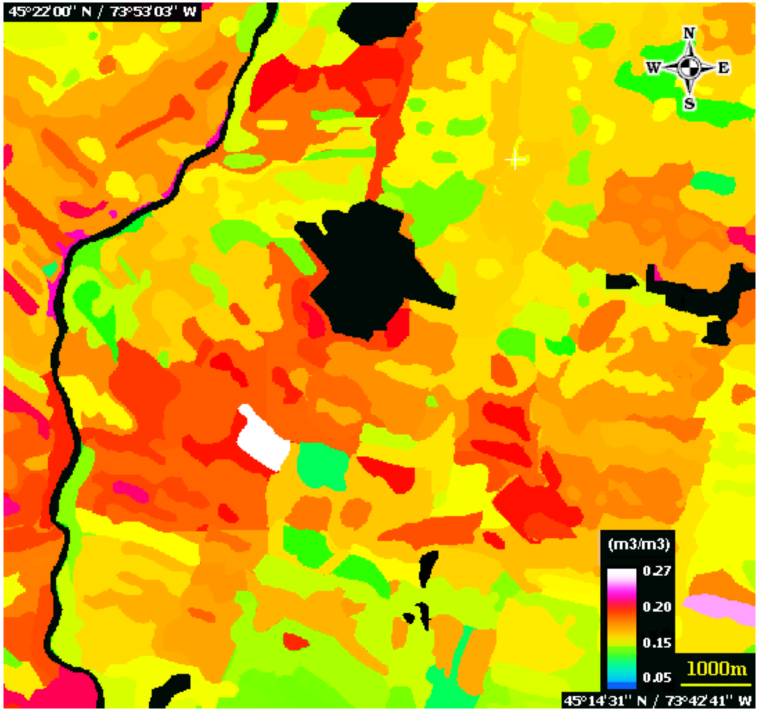

Fig. 14. Volumetric humidity map at homogeneous zone scale.

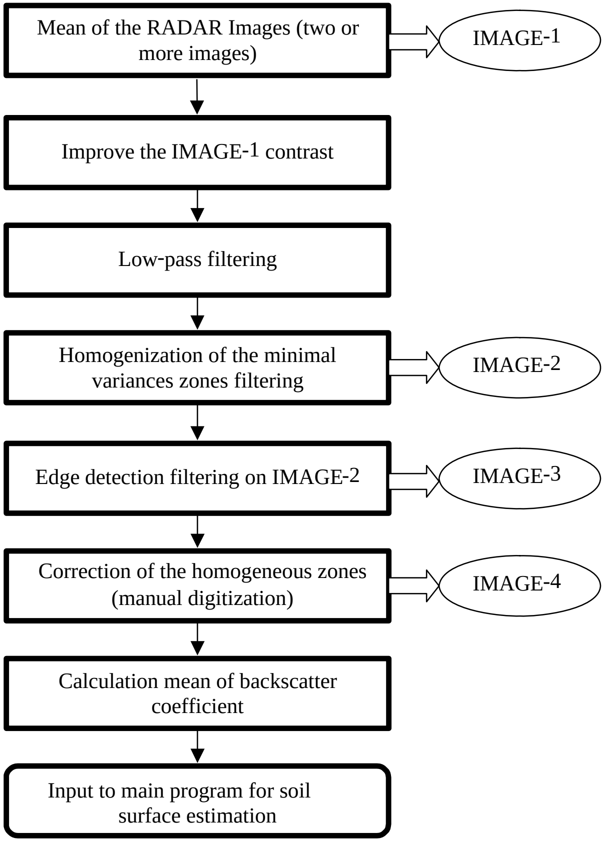

Fig. 15. Flowchart of homogeneous zone calculation.

HESSD

6, 207–241, 2009

Bare soil moisture and roughness estimation

M. R. Sahebi and J. Angles